Space-Resolved Modeling of Stationary Spots on Copper Vacuum Arc Cathodes and on Composite CuCr Cathodes with Large Grains

Mikhail S. Benilov, Mário D. Cunha, Werner Hartmann, Sylvio Kosse, Andreas Lawall, and Norbert Wenzel

***Abstract*— A self-consistent space-resolved numerical model of cathode spots in vacuum arcs is realized on the computational platform COMSOL Multiphysics. The model is applied to the investigation of stationary spots on planar cathodes made of copper or composite CuCr material with large ($\gtrsim$20 μm) chromium grains. The modeling results reveal a well defined spot with a structure, which is in agreement with the general theory of stationary cathode arc spots and similar to that of spots on cathodes of arcs in ambient gas. In the case of CuCr contacts with large chromium grains, spots with currents of the order of tens of amperes on copper coexist with spots on chromium with currents of the order of one or few amperes. The main effect of change of the cathode material from copper to chromium is a reduction of thermal conductivity of the cathode material, which causes a reduction of the radius of the spot and a corresponding reduction of the spot current.**

***Index Terms*— Cathode spots, circuit breakers, composite cathodes, vacuum arcs.**

I. Introduction

A VARIETY of approaches are available in the literature for modeling of cathode spots in vacuum arcs. These include space-resolved descriptions based on numerical solution of 1-D [1]–[5] or 2-D [6]–[12] partial differential equations, both stationary and nonstationary.

However, the simplest model, namely a stationary spot on an infinite planar cathode, has been studied mostly in the zero-dimensional approximation, where the spot is described only at the integral level ([13]–[16] and works referenced therein). Some authors have discussed the possibility of a thermal runaway, i.e., the instability caused by a positive feedback between Joule heat production in the cathode body and temperature because of the Wiedemann–Franz law [17], [18]. In mathematical terms, the presence of a thermal runaway would mean that a steady-state solution describing a stationary spot on an infinite planar vacuum arc cathode either does not exist or is unstable. Nonstationary zero-dimensional modeling performed in recent works [19]–[21] appears to indicate that a steady-state solution does exist and is stable. These works are interesting and useful, but they can hardly serve as the ultimate argument, i.e., a space-resolved 2-D modeling is required. The lack of a mathematically accurate solution of the most basic problem of the theory of plasma–cathode interaction in vacuum arc discharges is unfortunate and detrimental to the theory.

The aim of this and forthcoming papers is to obtain steady-state axially symmetric numerical solutions describing stationary spots on cathodes of vacuum arcs and to investigate their stability. Also investigated are the effect produced on these solutions and their stability by a granular structure of the cathode—a question that is of significant interest in connection with contacts of high-power vacuum circuit breakers.

Results reported in this paper concern steady-state solutions describing stationary spots on copper vacuum arc cathodes and cathodes made of CuCr composite material in which the chromium grains are large (no smaller than about 20 μm). Results on stability of these solutions, steady-state solutions describing stationary spots attached to small-to-medium size chromium grains, and stability of these solutions will be reported in a forthcoming paper.

The rest of this paper is structured as follows. The numerical model is described in Section II. Simulation results are given in Section III for spots on copper cathodes and in Section IV for spots on large chromium grains in a copper matrix. Conclusions are summarized in Section V.

II. Model of Individual Cathode Spots

A. Equations and Boundary Conditions

The model of plasma–cathode interaction used in this paper exploits the fact that significant power is deposited into the near-cathode space-charge sheath and is sometimes called the model of nonlinear surface heating. The model is widely used in the theory and modeling of arcs in ambient gas ([22] and works referenced therein, [23]–[27]). Distributions of temperature T and electrostatic potential φ in the cathode body

Manuscript received December 22, 2012; accepted February 11, 2013. Date of publication June 11, 2013; date of current version August 7, 2013. The work of Universidade da Madeira was supported by Fundação para a Ciência e a Tecnologia of Portugal through the Projects PTDC/FIS- PLA/2708/2012 Modelling, understanding, and controlling self-organization phenomena in plasma-electrode interaction in gas discharges: from first principles to applications and PEst-OE/MAT/UI0219/2011 Centro de Ciências Matemáticas and by Siemens AG.

M. S. Benilov and M. D. Cunha are with the Departamento de Física, CCCEE, Universidade da Madeira, Funchal 9000, Portugal (e-mail: benilov@uma.pt; mario@uma.pt).

W. Hartmann, S. Kosse, and N. Wenzel are with Siemens AG, Corporate Technology, Erlangen 91058, Germany (e-mail: werner.hartmann@siemens.com; sylvio.kosse@siemens.com; norbert.wenzel@siemens.com).

A. Lawall is with Siemens AG, Infrastructure & Cities, Low and Medium Voltage Division, Berlin 13629, Germany (e-mail: Andreas.Lawall@siemens.com).

Color versions of one or more of the figures in this paper are available online at http://ieeexplore.ieee.org.

Digital Object Identifier 10.1109/TPS.2013.2263255

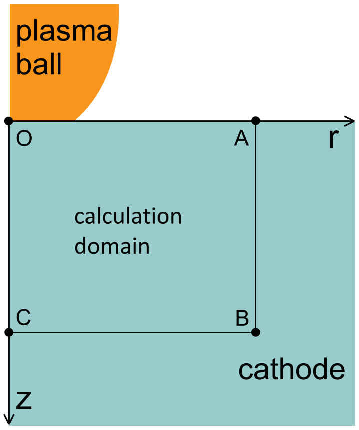

Fig. 1. Schematic of the model of a cathode spot.

are calculated by means of solving in the cathode body the time-dependent heat conduction equation, written with account of Joule heat generation in the cathode body, and the current continuity equation supplemented with Ohm's law

$$\rho_c c_p \frac{\partial T}{\partial t} = \nabla \cdot (\kappa \nabla T) + \sigma (\nabla \varphi)^2 \quad (1)$$

$$\nabla \cdot (\sigma \nabla \varphi) = 0. \quad (2)$$

Here, t is time, ρ_c, c_p, κ, and σ are, respectively, the mass density, specific heat, and thermal and electrical conductivities of the cathode material, which are treated as known functions of the local temperature: $\kappa = \kappa(T)$; $\rho_c = \rho_c(T)$; $c_p = c_p(T)$; and $\sigma = \sigma(T)$. Note that one can expect that the variation of potential inside the (metallic) cathode is small, and it will be seen that this is indeed the case. However, even small voltage drop in the cathode body can render the Joule effect inside the cathode quite significant [27].

Solutions shown hereafter have been computed for stationary spots on infinite planar cathodes (Fig. 1). The spots are axially symmetric and so is the modeling. Equations (1) and (2) are solved in a cylindrical domain designated $OABC$ in Fig. 1. Boundary conditions on the cathode surface (line OA) are $\kappa\, \partial T/\partial z = -q(T_w, U)$, $\sigma\, \partial\varphi/\partial z = -j(T_w, U)$, where q and j are densities of the energy flux and electric current from the plasma to the cathode surface computed in advance as functions of T_w, the local temperature of the cathode surface, and U, the near-cathode voltage drop; see the next section.

Boundary conditions far away from the spot (for $\rho \to \infty$, where $\rho = \sqrt{r^2 + z^2}$ is distance from the spot center) are $T \to T_\infty$, $\varphi \to 0$, where T_∞ is a known parameter (temperature of the cathode far away from the spot; results reported in this paper have been computed with $T_\infty = 1200$K). A straightforward numerical implementation would amount to setting $T = T_\infty$, $\varphi = 0$ on the boundary ABC. However, functions $(T - T_\infty)$ and φ decay for large ρ rather slowly: proportionally to ρ^{-1}, similarly to the potential of the electric field of a point charge. Therefore, the use of the straightforward boundary conditions would require the computation domain to be very large. It is natural in such a situation to apply on the boundary ABC somewhat more involved conditions

$$\rho \frac{\partial T}{\partial \rho} + T - T_\infty = 0, \quad \rho \frac{\partial \varphi}{\partial \rho} + \varphi = 0. \quad (3)$$

It can be readily verified that the functions on the LHS of (3) decay for $\rho \to \infty$ proportionally to ρ^{-2}, i.e., much faster than the functions $(T - T_\infty)$ and φ. Therefore, the use of conditions (3) allows us reduce the calculation domain compared to the case where the straightforward boundary conditions are used.

The current per spot, I, is expressed as $I = 2\pi \int_0^{r_A} j\,(T_w, U)\, r\, dr$, where r_A is the radius of the computation domain.

If the current per spot is specified, then the above-described nonlinear boundary-value problem is complete, the unknown quantities being functions $T(r, z)$, $\varphi(r, z)$, and parameter U. In this paper, this problem is numerically solved by means of the commercial software COMSOL Multiphysics. This software has been extensively used for modeling cathode spots in arcs in ambient gas [24], [25], [27]–[29]. The finite-volume mesh has to be strongly nonuniform because of a very fast variation of the density of the energy flux coming from the plasma which occurs in the vicinity of the spot edge. Note that, in some cases, the near-cathode voltage drop U was treated as a control parameter and the current per spot I as an unknown—a formulation of the problem that is mathematically equivalent as long as stationary spots are concerned but sometimes more convenient.

Note that one of the conditions of applicability of the considered model is that values of potential of the cathode surface be much smaller than the near-cathode voltage U; otherwise, the assumption of U being the same at different points of the cathode surface inside the spot and in its vicinity is unjustified.

Note that the above model may be readily adjusted for nonplanar cathodes, for example, cathode with micrometer-sized protrusions. It also allows one to investigate nonstationary effects, such as the formation of spots on a cathode of a given shape. On the other hand, the above formulation does not account for convective heat transfer due to the motion of molten metal and changes of shape of the cathode surface that may occur as a result of the motion of molten metal, microexplosions, and ejection of macroparticles.

B. Material Functions

Results reported in this paper refer to cathodes made of copper or chromium. Functions $q = q(T_w, U)$, $j = j(T_w, U)$ are evaluated using the model of near-cathode plasma layers in vacuum arcs, which is described in [30] and is based on a numerical simulation of near-cathode space-charge sheath with ionization of atoms emitted by the cathode surface [31]. Note that the dependence of q on T_w for a fixed U computed in [30] is nonmonotonic with a maximum, which is in agreement with a similar result [6] obtained on the basis of an elementary model. This is a very important feature, which is characteristic also of near-cathode layers in arcs in ambient gas and which suggests that spots on cathodes of vacuum arcs may appear as a result of instability of local thermal balance in a body heated by an external energy flux with a growing dependence on the local surface temperature and that stationary regimes of cathode spots in vacuum arcs are possible, at least in cases where the Joule heating inside the cathode is insignificant.

Thermal conductivity $\kappa(T)$ of copper is evaluated with the use of [32]. Note that the data in [32] cover the range up to 8500 K, although the values above 2600 K have been obtained by estimation. Thermal conductivity of chromium is evaluated with the use of [33] in the temperature range $T \lesssim 2000$ K and is assumed to be constant in the temperature range $T \gtrsim 2000$ K, where no data have been found.

Electrical conductivities $\sigma(T)$ of copper and chromium are evaluated in terms of the thermal conductivity $\kappa(T)$ using the Wiedemann–Franz law. Note that the data obtained in this way are in a good agreement with the data available in the literature [33]–[35] in the case of copper. Reference data are scarce in the case of chromium, but the agreement remains reasonably good.

III. Spots on Copper Cathodes

As an example, distributions of the temperature and potential in the cathode body for copper cathode and the near-cathode voltage of 20 V are shown in Fig. 2. Note that the electric current per spot, I, in this case equals 47 A. Distributions of different parameters over the cathode surface are shown in Fig. 3 for three values of the near-cathode voltage: $U = 20$ V, 18 V ($I = 61$ A), and 16 V ($I = 85$ A).

In each case, there is a well pronounced spot with a virtually constant temperature of the cathode surface, negligible current outside the spot, and a maximum of the density of energy flux from the plasma being positioned at the spot edge, which are features familiar from the general theory of stationary cathode arc spots [36] and from the modeling of spots on cathodes of arcs in ambient gas [37]. The maximum in the distribution of the density of energy flux over the cathode surface is a consequence of the above-mentioned nonmonotony of the dependence $q(T_w)$ for fixed U; therefore, the temperature at the spot edge coincides with the value of T_w corresponding to the maximum of the dependence $q(T_w)$. Maximum values of the temperature and potential occur at the cathode surface at the center of the spot. The electric current density, the erosion rate, and the ion backflow coefficient are virtually constant inside the spot, which is unsurprising since these quantities are evaluated in terms of the local surface temperature, which is also virtually constant. The electrostatic potential, which is not directly related to the surface temperature, varies appreciably inside the spot. The energy flux density, in spite of being evaluated in terms of the local surface temperature, also varies appreciably inside the spot, decreasing from the edge to the center, which is due to the extremely rapid decrease of the function $q(T_w)$ on the right-hand branch of the maximum. Again, this feature is well known from the general theory [36] and modeling of spots on cathodes of arcs in ambient gas [37]. The energy flux density outside the spot is small and negative: the plasma-related heating is absent since there is no plasma near the cathode surface outside the spot, so the cathode surface is cooled, mostly by the evaporation.

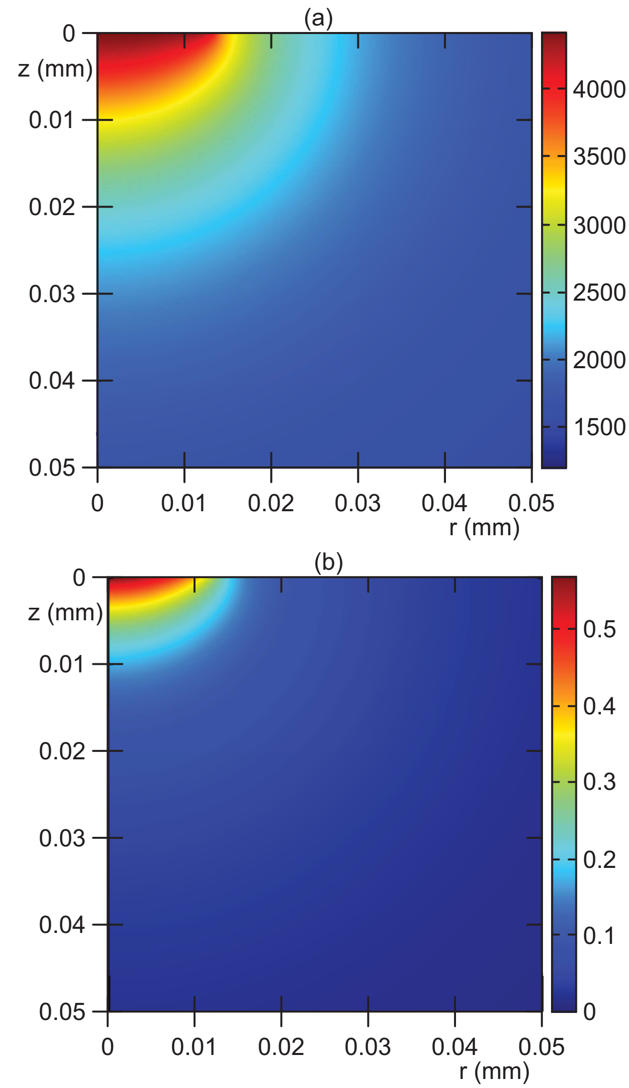

Fig. 2. Distributions of the temperature (a, in K) and potential (b, in V) in the cathode body. Coordinates in mm. Cu cathode, $U = 20$ V ($I = 47$ A).

Let us designate by T_* the value of T_w corresponding to the maximum of the dependence $q(T_w)$ and by T_2 the value of T_w at which the dependence $q(T_w)$ turns negative after passing through the maximum (or, in other words, the value starting from which the electron emission cooling exceeds the ion heating; see discussion in [30]). Strictly speaking, both values depend on U, but this dependence is weak: according to calculations [30], T_* varies from 4180 K for $U = 15$ V to 4130 K for $U = 20$ V, while T_2 equals 4420 K for all U from 15 to 20 V. The virtual constancy of T_* means that the temperature at the spot edge is virtually independent of U and, consequently, I. On the other hand, modeling in this paper has shown that the computed temperature of the cathode surface at the spot center, T_c, also is virtually constant and quite close to T_2: it varies between 4437 K for $U = 15$ V and 4407 K for $U = 20$ V.

The fact that the computed temperature at the center of a spot on a planar cathode is quite close to T_2 has already been known from modeling of cathode spots in arcs in ambient gas [37]. The difference is that the modeling [37] was

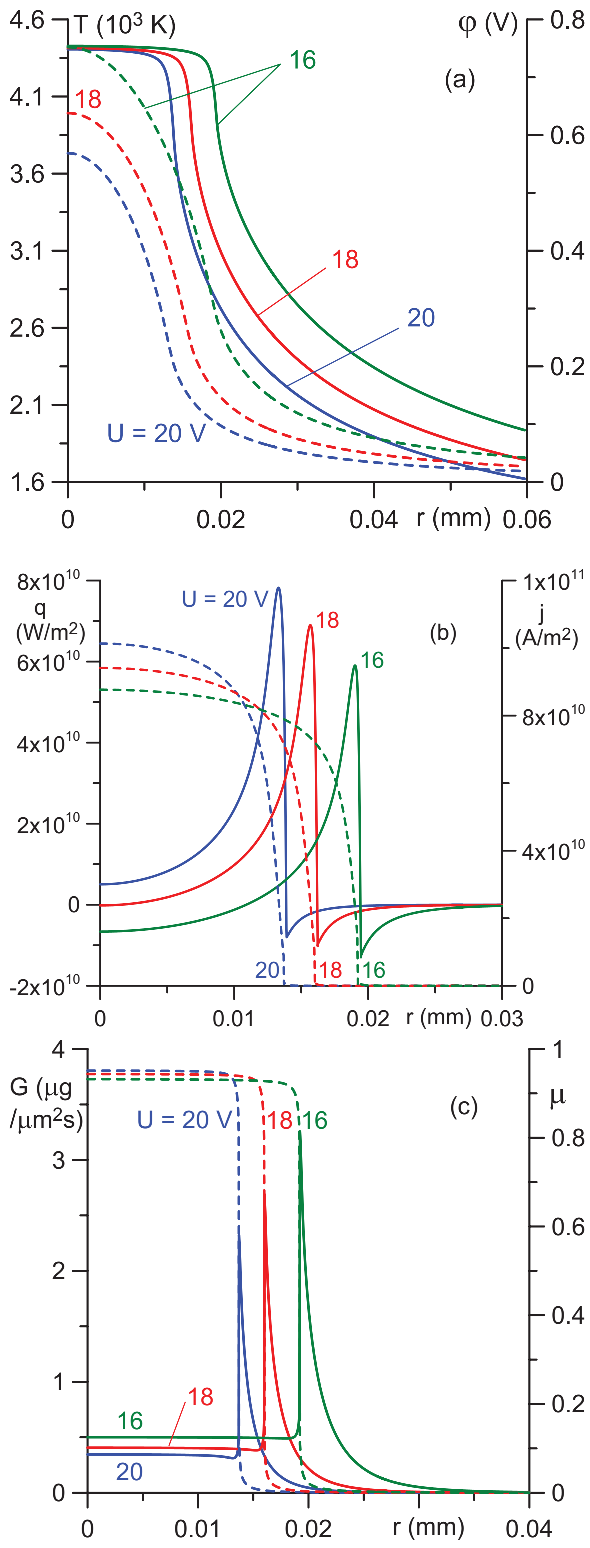

Fig. 3. Distributions of parameters over the surface of a copper cathode inside the spot and in its vicinity. (a) Temperature (solid) and potential (dashed). (b) Densities of energy flux (solid) and electric current (dashed) from the plasma to the cathode surface. (c) Erosion rate G (solid) and ion backflow coefficient μ (dashed).

performed without accounting for Joule heating inside the cathode body and, as a consequence, T_c never exceeded T_2. The present modeling takes into account Joule heating, and it is for this reason that situations are possible where $T_c > T_2$ and, as a consequence, the energy flux at the central part of the spot is negative, as shown by the distribution $q(r)$ for $U = 16$ V shown in Fig. 3(b). However, the difference $T_c - T_2$ is minimal, which is an obvious consequence of the modulus of the derivative $\partial q(T_w, U)/\partial T_w$ at $T_w = T_2$ being extremely high.

The above reasoning explains why the computed temperature of the cathode surface is virtually constant inside the spot and is virtually independent of the spot current, as seen in Fig. 3(a): these are consequences of T_* and T_2 being rather close (the difference $T_2 - T_*$ is in the range 240–290 K) and virtually independent of the near-cathode voltage drop. This reasoning also allows one to conveniently evaluate the temperature of the cathode surface inside a spot without actually simulating the spot (i.e., without performing numerical simulations described in Section II): it is sufficient to calculate the dependence of q on T_w and identify the temperatures T_* and T_2.

Inside the spot, the ion backflow coefficient μ is close to unity: most of the atoms emitted by the cathode surface get ionized in the space-charge sheath before the potential maximum [31] and return to the cathode in the form of ions. Outside the spot, the ion backflow coefficient is negligible. The erosion rate, while being nearly constant inside the spot, possesses a narrow maximum at the spot edge and tends to zero outside the spot. This is understandable if one takes into account the fact that the erosion rate represents a product of the evaporation rate and the escape factor $(1 - \mu)$. Outside the spot, the escape factor is close to unity; however, the temperature is low and the evaporation rate is negligible. Inside the spot, the evaporation rate is high but the escape factor is very low, so the erosion rate is not high. At the sheath edge, the evaporation rate is already rather high while the escape factor is still rather high, and the erosion rate attains a maximum value here. Note that this result is consistent with the nonmonotonic dependence of G on T_w discussed in [30].

Variations of potential in the cathode body are below 0.8 V in the current range considered, i.e., much smaller than the near-cathode voltage. This is an important result which, as mentioned at the end of Section II-A, justifies the model being employed.

Integral characteristics of spots on copper cathodes are plotted in Fig. 4 as functions of the current per spot. Here, $\varphi_c = \varphi(0, 0)$ is the potential of the cathode surface at the center of the spot; R is the spot radius estimated as the position of a point where the distribution of the energy flux density attains the maximum value; g is the so-called g-factor defined as the loss of mass of the cathode per unit charge transported (i.e., the integral loss of mass of the cathode per spot divided by the current per spot); Q_p is power per spot coming to the cathode surface from the plasma; and Q_J is power per spot dissipated in the cathode body due to Joule effect. Note that the loss of mass of the cathode and power Q_p coming from the plasma are found by integrating the quantities G and q over the cathode-surface boundary of the computation domain (line OA in Fig. 1), and power Q_J dissipated in the cathode

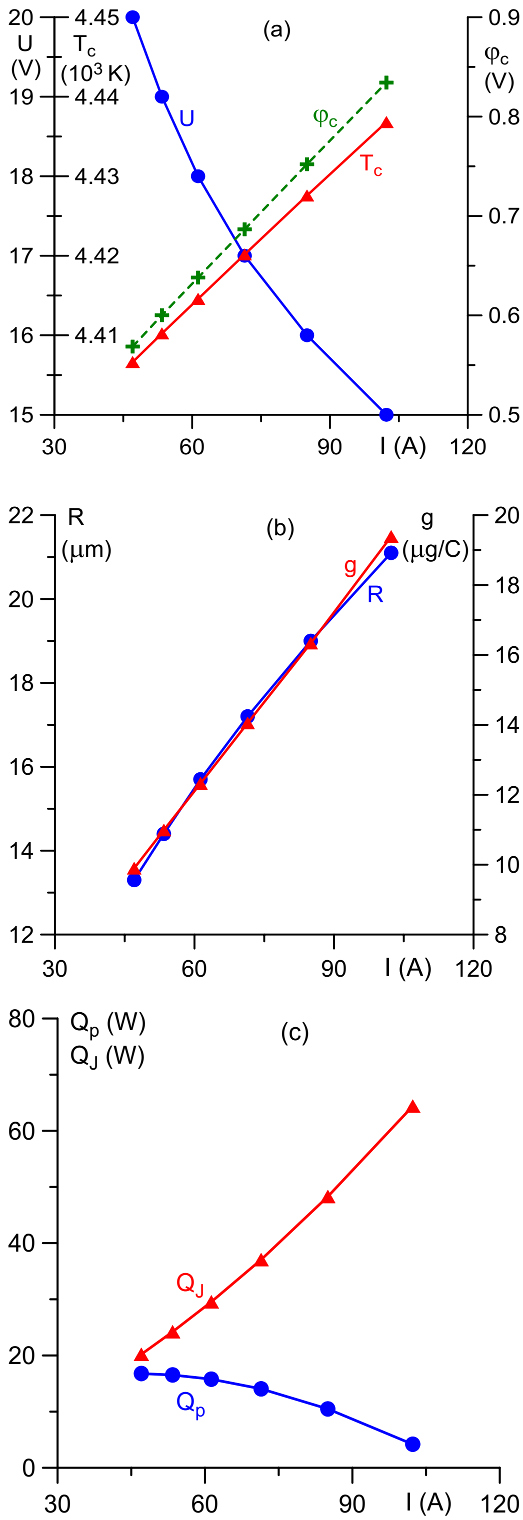

Fig. 4. Integral characteristics of spots on copper cathodes. (a) Near-cathode voltage U and the temperature and potential at the center of the spot, T_c and φ_c. (b) Spot radius R and erosion rate g. (c) Power coming from the plasma, Q_p, and power dissipated in the cathode body due to Joule effect, Q_J.

body is found by integrating the quantity $\sigma\,(\nabla\varphi)^2$ over the whole computation domain.

As the spot current increases from 47 to 102 A, the near-cathode voltage decreases from 20 to 15 V. The temperature at the center of the spot remains virtually constant as discussed above. Variation of potential in the cathode body slightly increases but remains under 0.9 V. The spot radius increases from 13 to 21 μm and the erosion rate increases from 10 to 19 μg/C.

The power Q_p coming from the plasma decreases from 17 to 4 W. This power represents only a small fraction of the total power IU deposited by the external circuit into the near-cathode plasma layer, which varies from 941 to 1534 W. It follows that most part of the deposited power is transported from the near-cathode layer into the bulk plasma by the electric current and flux of the erosion products. The power Q_J dissipated in the cathode body due to Joule effect exceeds the power coming from the plasma and increases from 20 to 64 W.

A quantitative comparison of the above numerical solutions with experiment is unwarranted before one can be sure that the above solutions are stable and therefore may be realized. It is worth noting, however, that the computed parameters fit into the usual range of parameters of macrospots, or group spots [38]. Values of g-factor shown in Fig. 4(b), which refer to the ion erosion rate, represent about one-fourth to one-half of the experimental values of the ion erosion g-factor for copper, which are in the range 33–39 μg/C [39, p. 157]. This may indicate that the vaporization mechanism is responsible for about one-fourth to one-half of the ion erosion and the rest is due to explosive emission [40].

IV. Spots on Large Cr Grains in Cu Matrix

This section is concerned with spots on cathodes made of CuCr composite material in which the Cr grains are large, which occurs at initial stages of life of contacts of high-power vacuum circuit breakers. The analytical treatment in [30] has shown that, in this case, spots with currents of the order of tens of amperes on copper coexist with spots on chromium with currents of the order of 1 A or a few amperes. In this connection, integral characteristics of spots on chromium cathodes computed numerically as described in Section II are shown in Fig. 5 for near-cathode voltages from 15 to 20 V, which correspond to spots with current of the order of tens of amperes on copper as seen in Fig. 4(a). One can see that spots on chromium operate at currents between 1.9 and 3.6 A according to the numerical simulations, which is in agreement with the prediction of the analytical treatment [30]. The temperatures at the center of the spot on copper and chromium cathodes are similar, but the spot radius and the erosion rate are smaller on chromium—again effects predicted by the analytical treatment [30]. Variations of potential in the cathode body are smaller for chromium. Power coming from the plasma to a spot on chromium is significantly smaller than that coming to a spot on copper. On the other hand, power coming from the plasma to a spot on chromium exceeds that dissipated inside the cathode. The g-factor of spots on copper exceeds that of spots on chromium by a factor of about 2. Taking into account strongly differing currents, one concludes that the rate of ion erosion of copper exceeds that of chromium by up to two orders of magnitude—again a result predicted by the analytical treatment [30].

As pointed out in [30], because of low current, small diameter, and low erosion rate, spots on chromium should be much dimmer than those on copper and are not easy to observe. However, high-resolution photographs of copper–chromium contacts of high-current arcs [41]–[43] have revealed, in addition to cathode spots with the average current of 45 A similar to those on pure copper cathodes, also very small and dim spots. The latter may be interpreted as the spots on chromium predicted by the analytical treatment [30] and the numerical modeling in this paper. Consistent with this interpretation is the well established experimental fact that the value of the chopping current is of the order of few amps on CuCr contacts (and on contacts made of copper with other additives) and of the order of 10A on pure copper contacts [44]–[48].

In order to understand the reason for such a large difference between spots on copper and chromium, modeling has been performed of spots on cathodes with "mixed" material functions. Integral characteristics of spots obtained in these simulations are shown in Table I for $U = 20$ V. (Data in the second and last lines of Table I refer to "unmixed" material functions corresponding to chromium and copper, respectively, and have been added for comparison; data shown in the third line, which is marked Cu Cr Cr, have been obtained by means of simulations with the electrical conductivity of the cathode material referring to Cu, thermal conductivity referring to Cr, and the pair of functions $q\,(T_w, U)$, $j\,(T_w, U)$, characterizing the plasma–cathode interface, referring to Cr; etc.) One can see that the switching in each of the material functions from Cr to Cu causes an increase of current, the increase caused by the switching in thermal conductivity being the strongest.

One can invoke the general theory of stationary cathode arc spots [36] in order to understand these effects, although it should be kept in mind that this theory neglects the Joule effect in the cathode body. In the framework of this theory, the spot radius is governed by the following formula that has been derived by means of asymptotic solution of the equation of heat conduction in the cathode body:

$$R = \frac{1}{\pi}\left[\int_{T_\infty}^{T_*} \varkappa\,(T)\;dT\right]^2 \left\{\int_{T_\infty}^{T_2} q\,(T, U)\;\varkappa\,(T)\;dT\right\}^{-1}. \tag{4}$$

Given that the temperatures at the spot center are quite close for all variants shown in Table I, one should assume that the current densities in the spot are close as well. The latter leads one to the assumption that the spot current in the transition between the variants varies approximately proportionally to R^2, and one can see from Table I that this is indeed the case. Thermal conductivity of copper in the temperature range of interest exceeds that of chromium by a factor of about 3. It follows that the switching of thermal conductivity from chromium to copper should cause an increase in R by about 3 and in I by about an order of magnitude. Comparing variants (Cr, Cr, Cr) and (Cr, Cu, Cr) in Table I, and also variants (Cu, Cr, Cr) and (Cu, Cu, Cr), one can check that this is indeed the case. Note that the increase in R seen in the transition from the variant (Cu, Cu, Cr) to (Cu, Cu, Cu) in Table I is consistent with the integral in the curly brackets on the RHS of (4), when evaluated with the use of the function

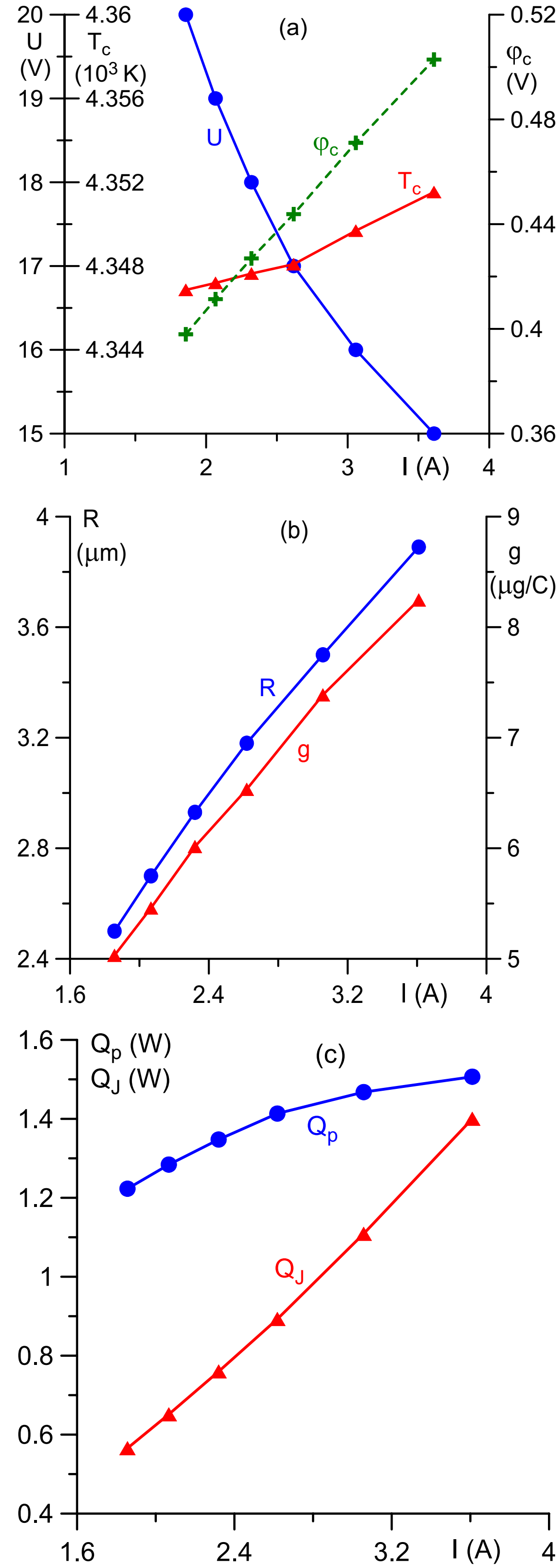

Fig. 5. Integral characteristics of spots on chromium cathodes. Designations are the same as in Fig. 4.

q for copper, being smaller than that evaluated with the use of the function q for chromium (see Fig. 6(a) [30]).

One can conclude that the significant difference in integral parameters of spots on copper and chromium is due in the

TABLE I
EFFECT OF MATERIAL FUNCTIONS ON INTEGRAL PARAMETERS OF SPOTS. $U = 20$V

$\sigma(T)$	$\kappa(T)$	$q(T_w, U)$, $j(T_w, U)$	I (A)	T_c (K)	φ_c (V)	R (μm)	Q_p (W)	Q_J (W)
Cr	Cr	Cr	1.9	4347	0.4	2.5	1.2	0.56
Cu	Cr	Cr	2.6	4340	0.13	3	1.7	0.26
Cr	Cu	Cr	13.7	4381	1.23	6.4	6.5	12.7
Cu	Cu	Cr	27.9	4356	0.46	9.5	15.3	9.7
Cu	Cu	Cu	47	4407	0.57	13.3	16.8	20.2

first place to different thermal conductivities of copper and chromium.

One can see from Fig. 5(b) that the diameter of spots on chromium is up to approximately 8 μm. This allows one to specify the limit of validity of the present modeling as far as the Cr grain size is concerned: it should be no smaller than about 20 μm.

V. CONCLUSION

A space-resolved numerical model of cathode spots in vacuum arcs has been realized on the computational platform COMSOL Multiphysics. The approach is based on the model of nonlinear surface heating, which is widely used in the theory and modeling of plasma–cathode interaction in arcs in ambient gas, supplemented with a module simulating near-cathode layers in vacuum arcs. The model allows one to compute both stationary and nonstationary spots on cathodes of any given shape. Results reported in this paper concern stationary spots on planar cathodes made of copper or composite CuCr material with large ($\gtrsim 20$ μm) chromium grains.

In every case, there is a well pronounced spot with a virtually constant temperature of the cathode surface and a maximum of the density of energy flux from the plasma being positioned at the spot edge. The spot structure is in agreement with the general theory of stationary cathode arc spots and similar to that of spots on cathodes of arcs in ambient gas.

In the case of CuCr contacts with large chromium grains, which occurs at the initial stages of life of contacts of high-power circuit breakers, independent spots operate on the copper matrix and chromium grains at the same value of the near-cathode voltage. The modeling results indicate, in agreement with the analytical treatment [30], that spots with current of the order of tens of amperes on copper coexist with spots on chromium with currents of the order of one or few amperes. It is found that the main effect of change of the cathode material from copper to chromium is a reduction of the thermal conductivity of the cathode material, which causes a reduction of the radius of the spot and a corresponding reduction of the spot current.

REFERENCES

[1] E. A. Litvinov, G. A. Mesyats, and A. G. Parfenov, "The nature of explosive electron emission," *Soviet Phys. Doklady*, vol. 28, no. 3, pp. 272–273, 1983.

[2] E. A. Litvinov, G. A. Mesyats, and A. G. Parfenov, "The origin of the cyclical nature of explosive electron emission," *Soviet Phys. Doklady*, vol. 29, no. 12, pp. 1019–1020, 1984.

[3] J. Prock, "Time-dependent description of cathode crater formation in vacuum arcs," *IEEE Trans. Plasma Sci.*, vol. 14, no. 4, pp. 482–491, Aug. 1986.

[4] J. Mitterauer and P. Till, "Computer simulation of the dynamics of plasma-surface interactions in vacuum arc cathode spots," *IEEE Trans. Plasma Sci.*, vol. 15, no. 5, pp. 488–501, Oct. 1987.

[5] T. Klein, J. Paulini, and G. Simon, "Time-resolved description of cathode spot development in vacuum arcs," *J. Phys. D, Appl. Phys.*, vol. 27, no. 9, p. 1914, 1994.

[6] M. S. Benilov, "Nonlinear heat structures and arc-discharge electrode spots," *Phys. Rev. E*, vol. 48, no. 1, pp. 506–515, 1993.

[7] Z.-J. He and R. Haug, "Cathode spot initiation in different external conditions," *J. Phys. D, Appl. Phys.*, vol. 30, no. 4, pp. 603–613, 1997.

[8] D. L. Shmelev and E. A. Litvinov, "The computer simulation of the vacuum arc emission center," *IEEE Trans. Plasma Sci.*, vol. 25, no. 4, pp. 533–537, Aug. 1997.

[9] R. Schmoll, "Analysis of the interaction of cathode microprotrusions with low-temperature plasmas," *J. Phys. D, Appl. Phys.*, vol. 31, no. 15, p. 1841, 1998.

[10] D. L. Shmelev and E. A. Litvinov, "Computer simulation of ecton in a vacuum arc," *IEEE Trans. Dielectr. Electr. Insul.*, vol. 6, no. 4, pp. 441–444, Aug. 1999.

[11] I. V. Uimanov, "A two-dimensional nonstationary model of the initiation of an explosive center beneath the plasma of a vacuum arc cathode spot," *IEEE Trans. Plasma Sci.*, vol. 31, no. 5, pp. 822–826, Oct. 2003.

[12] S. A. Barengolts, G. A. Mesyats, and M. M. Tsventoukh, "Initiation of ecton processes by interaction of a plasma with a microprotrusion on a metal surface," *JETP*, vol. 107, no. 6, pp. 1039–1048, 2008.

[13] V. I. Rakhovsky, "State of the art of physical models of vacuum arc cathode spots," *IEEE Trans. Plasma Sci.*, vol. 15, no. 5, pp. 481–487, Oct. 1987.

[14] I. Beilis, "Theoretical modeling of cathode spot phenomena," in *Handbook of Vacuum Arc Science and Technology: Fundamentals and Applications*, R. L. Boxman, D. M. Sanders, and P. J. Martin, Eds. Park Ridge, NJ, USA: Noyes, 1995, pp. 208–256.

[15] I. I. Beilis, "State of the theory of vacuum arcs," *IEEE Trans. Plasma Sci.*, vol. 29, no. 5, pp. 657–670, Oct. 2001.

[16] I. I. Beilis, "Wall interactions with plasma generated by vacuum arcs and targets irradiated by intense laser beams," *Plasma Sour. Sci. Technol.*, vol. 18, no. 1, pp. 014015-1–014015-16, 2009.

[17] E. Hantzsche, "Thermal runaway prevention in arc spots," *IEEE Trans. Plasma Sci.*, vol. 11, no. 3, pp. 115–122, Sep. 1983.

[18] E. Hantzsche, "Mysteries of the arc cathode spot: A retrospective glance," *IEEE Trans. Plasma Sci.*, vol. 31, no. 5, pp. 799–808, Oct. 2003.

[19] I. I. Beilis, "The nature of high voltage initiation of an electrical arc in a vacuum," *Appl. Phys. Lett.*, vol. 97, no. 12, pp. 121501-1–121501-3, Sep. 2010.

[20] I. I. Beilis, "Continuous transient cathode spot operation on a microprotrusion: Transient cathode potential drop," *IEEE Trans. Plasma Sci.*, vol. 39, no. 6, pp. 1277–1283, Jun. 2011.

[21] I. I. Beilis, "Cathode spot development on a bulk cathode in a vacuum arc," in *Proc. 25rd Int. Symp. Discharges Electr. Insul. Vacuum*, vol. 2. Sep. 2012, pp. 365–368.

[22] M. S. Benilov, "Understanding and modelling plasma-electrode interaction in high-pressure arc discharges: A review," *J. Phys. D, Appl. Phys.*, vol. 41, no. 14, pp. 144001-1–144001-30, Jul. 2008.

[23] J. J. Gonzalez, F. Cayla, P. Freton, and P. Teulet, "Two-dimensional self-consistent modelling of the arc/cathode interaction," *J. Phys. D, Appl. Phys.*, vol. 42, no. 14, p. 145204, Jul. 2009.

[24] A. Bergner, M. Westermeier, C. Ruhrmann, P. Awakowicz, and J. Mentel, "Temperature measurements at thoriated tungsten electrodes in a model lamp and their interpretation by numerical simulation," *J. Phys. D, Appl. Phys.*, vol. 44, no. 50, p. 505203, Dec. 2011.

[25] M. S. Benilov, L. G. Benilova, H.-P. Li, and G.-Q. Wu, "Sheath and arc-column voltages in high-pressure arc discharges," *J. Phys. D, Appl. Phys.*, vol. 45, no. 35, p. 355201, Sep. 2012.

[26] M. Baeva, R. Kozakov, S. Gorchakov, and D. Uhrlandt, "Two-temperature chemically non-equilibrium modelling of transferred arcs," *Plasma Sour. Sci. Technol.*, vol. 21, no. 5, p. 055027, Oct. 2012.

[27] M. S. Benilov and M. D. Cunha, "Joule heat generation in thermionic cathodes of high-pressure arc discharges," *J. Appl. Phys.*, vol. 113, no. 6, pp. 063301-1–063301-11, Feb. 2013.

[28] L. Dabringhausen, O. Langenscheidt, S. Lichtenberg, M. Redwitz, and J. Mentel, "Different modes of arc attachment at HID cathodes: Simulation and comparison with measurements," *J. Phys. D, Appl. Phys.*, vol. 38, no. 17, pp. 3128–3142, Sep. 2005.

[29] M. S. Benilov, M. D. Cunha, and M. J. Faria, "Simulating different modes of current transfer to thermionic cathodes in a wide range of conditions," *J. Phys. D, Appl. Phys.*, vol. 42, no. 14, pp. 145205-1–145205-17, Jul. 2009.

[30] N. A. Almeida, M. S. Benilov, L. G. Benilova, W. Hartmann, and N. Wenzel, "Near-cathode plasma layer on CuCr contacts of vacuum arcs," *IEEE Trans. Plasma Sci.*, vol. 41, no. 8, pp. 1938–1949, Aug. 2013.

[31] M. S. Benilov and L. G. Benilova, "The double sheath on cathodes of discharges burning in cathode vapour," *J. Phys. D, Appl. Phys.*, vol. 43, no. 34, pp. 345204-1–345204-12, 2010.

[32] Y. S. Touloukian, R. W. Powell, C. Y. Ho, and P. G. Clemens, *Thermal Conductivity. Metallic Elements and Alloys* (Thermophysical Properties of Matter), vol. 1. New York, NY, USA: Plenum, 1970.

[33] D. R. Lide, *CRC Handbook of Chemistry and Physics*, 84th ed. Boca Raton, FL, USA: CRC Press, 2004.

[34] I. S. Grigoriev and E. Z. Meilikhov, *Handbook of Physical Quantities*. Boca Raton, FL, USA: CRC Press, 1997.

[35] W. F. Gale and T. C. Totemeier, *Smithells Metals Reference Book*, 8th ed. Amsterdam, The Netherlands: Elsevier, 2004.

[36] M. S. Benilov, "Maxwell's construction for non-linear heat structures and determination of radius of arc spots on cathodes," *Phys. Scripta*, vol. 58, no. 4, pp. 383–386, 1998.

[37] M. S. Benilov and M. D. Cunha, "Heating of refractory cathodes by high-pressure arc plasmas: II," *J. Phys. D, Appl. Phys.*, vol. 36, no. 6, pp. 603–614, Mar. 2003.

[38] B. Jüttner, "Cathode spots of electric arcs," *J. Phys. D, Appl. Phys.*, vol. 34, no. 17, pp. 103–123, 2001.

[39] A. Anders, *Cathodic Arcs: From Fractal Spots to Energetic Condensation* (Springer Series on Atomic, Optical, and Plasma Physics). New York, NY, USA: Springer-Verlag, 2008.

[40] G. A. Mesyats and S. A. Barengol'ts, "Generation mechanism of anomalous ions in vacuum arcs," *Phys. Uspekhi*, vol. 45, no. 10, pp. 1001–1018, 2002.

[41] W. Hartmann, A. Lawall, R. Renz, N. Wenzel, and W. Wietzorek, "Experimental investigations on cathode spots and dynamical vacuum arc structure in an axial magnetic field," in *Proc. 23rd Int. Symp. Discharges Electr. Insul. Vacuum*, vol. 1. Sep. 2008, pp. 259–263.

[42] W. Hartmann, A. Lawall, R. Renz, N. Wenzel, and W. Wietzorek, "Cathode spots and arc structure in a dense, axial magnetic field-stabilised vacuum arc," in *Proc. 24th Int. Symp. Discharges Electr. Insul. Vacuum*, Sep. 2010, pp. 245–248.

[43] W. Hartmann, A. Lawall, R. Renz, M. Romheld, N. Wenzel, and W. Wietzorek, "Cathode spot dynamics and arc structure in a dense axial magnetic-field-stabilized vacuum arc," *IEEE Trans. Plasma Sci.*, vol. 39, no. 6, pp. 1324–1329, Jul. 2011.

[44] W. F. Rieder, M. Schussek, W. Glatzle, and E. Kny, "The influence of composition and CR particle size of CU/CR contacts on chopping current, contact resistance, and breakdown voltage in vacuum interrupters," *IEEE Trans. Compon. Hybrids Manuf. Technol.*, vol. 12, no. 2, pp. 273–283, Jun. 1989.

[45] W. Hartmann, L. Kellmann, R. Renz, K.-D. Rohde, and N. Wenzel, "Kontaktwerkstoffe und prüfverfahren in der vakuumschalttechnik," in *Albert-Keil-Kontaktseminar Kontaktverhalten und Schalten*. Berlin, Germany: Springer-Verlag, Sep. 1999, pp. 191–196.

[46] C. Ding, S. Yanabu, and S. Arai, "Instability and chopping phenomena of a low-current vacuum arc," *Electr. Eng. Jpn.*, vol. 145, no. 4, pp. 12–19, 2003.

[47] Z. Yang, Q. Zhang, Q. Wang, C. Zhang, and B. Ding, "Vacuum arc characteristics on nanocrystalline CuCr alloys," *Vacuum*, vol. 81, no. 4, pp. 545–549, 2006.

[48] P. Halbach, K. Golde, V. Hinrichsen, K. Ermeler, and J. Teichmann, "Switching behavior of vacuum interrupters under practical system conditions," in *Proc. 24th Int. Symp. Discharges Electr. Insul. Vacuum*, Sep. 2010, pp. 253–256.

Mikhail S. Benilov received the Diploma degree (Hons.) and the C.Sc. (Ph.D.) degree in physics from the Moscow Institute for Physics and Technology, Moscow, Russia, in 1974 and 1978, respectively, and the Doctor of Physical and Mathematical Sciences degree from the Institute for High Temperatures, USSR Academy of Sciences, Moscow, in 1990. His thesis focuses on theory of electrostatic probes and electrodes in high-pressure flowing plasmas.

He had been with the Institute for High Temperatures, USSR Academy of Sciences, Moscow, where he led a group working in plasma and nonlinear physics, numerical modeling, and fluid dynamics, after completing postgraduate courses with the Moscow Institute for Physics and Technology and Institute for Mechanics of Lomonosov Moscow State University, Moscow, in 1977. Since 1993, he has been a Professor and a Chair with the Department of Physics, University of Madeira. His current research interests include plasma physics, in particular, plasma-electrode interaction, nonlinear physics, and numerical modeling.

Dr. Benilov received the Alexander von Humboldt Research Fellowship in 1990 and stayed for two years with the Ruhr-Universität Bochum, Germany, working on the theory and simulation of near-electrode phenomena.

Mário D. Cunha received the Ph.D. degree in physics from the University of Madeira, Madeira, Portugal, in 2004. His thesis focused on the modeling of the plasma-cathode interaction in high-pressure arc discharges.

He is an Assistant Professor with the Department of Physics, University of Madeira. His current research interests include numerical simulation of different modes of current transfer to cathodes of high-pressure arc discharges, and also spots on vacuum arc cathodes.

Werner Hartmann received the M.S. degree in physics in 1981 from the University of Erlangen, Erlangen, Germany, where he received the Ph.D. degree in 1986.

He has been with Siemens Corporate Technology, as a Researcher, Research Group Leader, Project Manager, and as a Program Manager, since 1991. He was a Research and Teaching Assistant with the University of Erlangen, Physics Department, from 1986 to 1991, and with the University of Southern California, Los Angeles, CA, USA, in 1987 and 1988, where he conducted research on cold cathode thyratrons/pseudosparks and fast dynamic z-pinches as EUV light sources. He was responsible for fundamental and applied research into vacuum switching arc physics and devices at the Corporate Technology of Siemens, being involved in the development of low voltage contactors, low voltage circuit breakers up to 130 kA breaking capacity, medium voltage vacuum circuit breakers, and the successful development of high voltage vacuum circuit breakers for 72 and 145 kV. He was involved in the development of a fully 3-D, fully transient software code for the simulation of low voltage switching arcs in air as a Project Manager. He developed environmental and environmentally friendly technologies for industrial applications, mainly in the areas of clean water, clean air, and electroporation. Since 2006, his research interests have been in the field of mining applications, particularly in the field of flotation and magnetic separation. Currently, he holds the position of a Senior Key Expert in the area of environmental technologies.

Sylvio Kosse received the Diploma and Doctoral degrees in theoretical physics from Greifswald University, Greifswald, Germany, in 1996 and 2002, respectively.

He is currently with Siemens AG, Corporate Technology, Munich, Germany, and is Head of the research group Renewable Energy and Grid Solutions.

Andreas Lawall was born in Germany in 1971. He received the Dipl.-Phys. degree from the Technical University of Berlin, Berlin, Germany, in 1999.

He joined Siemens AG in 2003 as a Developer and a Project Leader for vacuum interrupters. His current interests include closing the gap between basic research and commercial products.

Mr. Lawall is a member of the German Physical Society.

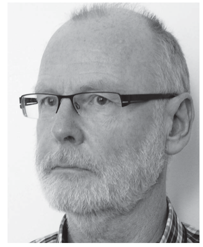

Norbert Wenzel received the M.Ed. degree in physics and mathematics from the University of Heidelberg, Heidelberg, Germany, in 1979, and the Ph.D. degree in physics with the same institution in 1985.

He has been with Siemens Corporate Technology as a Researcher, Test Laboratory Head, Project Leader, and as a Radiation Protection Officer since 1985. From 1978 to 1985, he was a Research and Teaching Assistant with the University of Heidelberg, Department of Applied Physics, and with the Institute of Plasma Research, University of Stuttgart, Stuttgart, Germany, on fusion-oriented plasma physics and plasma diagnostics. In 1982, he held a EURATOM fellowship with the Nuclear Fusion Research Center of the Association ENEA in Frascati, Rome, Italy. From 1985 to 1992, he applied nonlinear Raman spectroscopic techniques to industrial processes, such as low voltage air breakers and gas lasers. He was responsible for the development of sealed-off carbon dioxide slab lasers excited by radio-waves and microwaves. Since 1992, he has been working in the field of fundamental and applied research of switching arcs with the Corporate Technology of Siemens. As the Head of a Synthetic Test Laboratory, he was involved in the development of low and medium voltage vacuum interrupters up to 130 kA breaking capacity and the development of high voltage vacuum circuit breakers for 72 and 145 kV. Since 2006, he has been extending his field of activities to the physical modeling and numerical simulation of arc plasmas taking into account cathode surface phenomena. He developed a transient, 3-D simulation software to describe the evolution of vacuum switching arcs in axial magnetic field contacts. Currently, he holds the position of Senior Key Expert Research Scientist in the area of switching technologies.